Progress In Electromagnetics Research Letters, Vol. 95, 135–141, 2021

A Slotted Patch Antenna with Enhanced Gain Pattern for Automotive Applications

Stefano Maddio, Giuseppe Pelosi, Monica Righini, and Stefano Selleri*

Abstract—A single-layer via-less rectangular patch antenna for automotive applications in C-band is proposed. To match the needs of a vehicular dedicated short range communication protocol, the resonant edge of the antenna is enlarged to narrow the beamwidth in the H-plane, while at the same time a pair of thin slots serve as inhibitors for the higher modes, permitting adequate matching and polarization purity. The proposed single patch antenna presents a realized gain about 6.85 dB, H-plane beamwidth narrower than $\pm 32°$, E-plane beamwidth larger than $\pm 45.5°$, and return loss exceeding 20 dB with a 3 dB bandwidth of 500 MHz, with a minimum at 5810 MHz, hence suitable for coexistence of different communication standard in the C-band. Furthermore, its compact dimension permits the direct integration within a radio front-end.

1. INTRODUCTION

There is a great moment about Intelligent Transportation System (ITS), the vehicular communication framework for safety and services working in the C-band. Alongside the dedicated short range communication (DSRC protocol at 5.8 GHz), there is WAVE protocol, based on 802.11p WiFi at 5.9 GHz. In Italy, according to the ETSI standard [1], the fixed and mobile nodes are linearly polarized.

With reference to [2], for Electronic Toll Collection (ETC) applications, a typical mobile node is a very low-cost passive device, which operates in back-scattering, and its functioning is guaranteed by the impinging power from the Road-Side Unit. Therefore, the gain performance of the antenna is of paramount importance for communication success [3].

The geometry of the link suggests to have a wide half power beamwidth (HPBW) in the E-plane, to grant the link for a wide angle of view alongside the roadway, but with a narrow HPBW in the H-plane, adequate to cover only the width of a single lane [4, 5]. Typically, the array based solution, even with a few elements, while guaranteeing the pattern specifications, is not practical due to its size or, at least, very challenging [6].

To address this problem, in this paper we present a compact, uniplanar, patch antenna. The idea is to enlarge the resonant edge so as to shape the beam according to the above mentioned needs, while maintaining a compact structure with a single feed point and without the distribution network of an array. To match specifications, with a single patch, two slots are etched on the patch itself to suppress undesired higher modes. Etching slots in a patch is well known to have effects on the patch current distribution, and there are many recent applications in which slots are used to tune these currents to a desired behavior [7, 8].

2. ANTENNA DESIGN

Figure 1 shows the basic geometry of an antenna element, which consists of a rectangular patch $L_p \times W_p$, etched on a dielectric substrate having a height of h_s and a dielectric constant of ε_r.

Received 1 November 2020, Accepted 28 December 2020, Scheduled 5 January 2021

* Corresponding author: Stefano Selleri (stefano.selleri@unifi.it).

The authors are with the Department of Information Engineering, University of Florence, Via di S. Marta, 3, 50139 Florence, Italy.

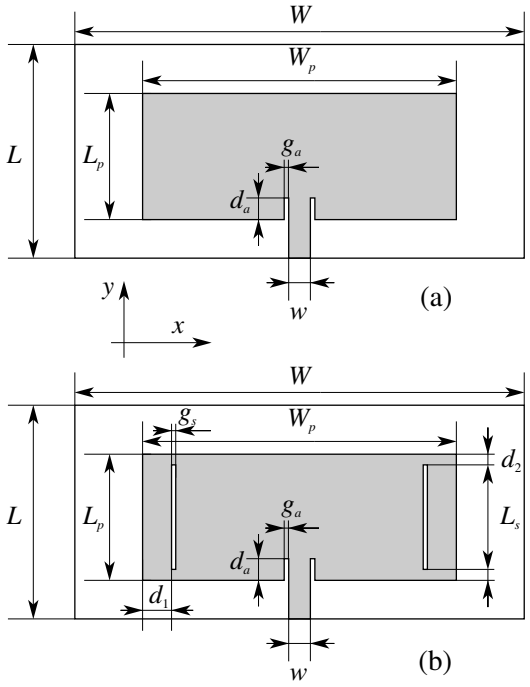

Figure 1. (a) Geometry of a conventional center-fed single-layer rectangular patch antenna (this layout, with different dimensions, will be, in the following, the one of patch p#1 and p#2); (b) proposed geometry of the patch with slots (this layout will be, in the following, the one of patch p#3).

As well known, a patch antenna is a resonant antenna whose operative frequency can be roughly estimated via the well-known cavity model [9, 10]. Cavity modes theoretically depend on three integers but, for a patch antenna, modes having a field dependency on the thickness of the substrate are too high in frequency to be relevant, hence just 2D resonances are considered, with two indexes m, n, and the pertinent resonant frequencies are f_{mn}:

$$f_{mn} = \frac{1}{2\pi\sqrt{\varepsilon\mu}}\sqrt{\left(\frac{m\pi}{W_p}\right)^2 + \left(\frac{n\pi}{L_p}\right)^2} \tag{1}$$

where ε and μ being the absolute permittivity and permeability of the substrate, respectively.

The first mode, if $W_p > L_p$ as in Figure 1(a), is TM_{10}. Anyway if the feed is positioned as in Figure 1, at the midpoint of the longer side, mode TM_{10} cannot be excited for symmetry reasons, hence the first excited and radiating mode is indeed TM_{01}. This is true as long as $L_p < W_p < 2L_p$. As W_p approaches the $2L_p$ limit, the resonant frequency of the p-dependent modes becomes smaller and smaller. For $W_p = 2L_p$, TM_{01} and TM_{20} show the same theoretical resonant frequency, so they degenerate, and the latter can be excited by the feed shown in Figure 1. This fixes a limit on the maximum size of the radiating (W_p-long) edge of a rectangular patch antenna and, as a consequence, on the achievable maximum realized gain. If $W_p > 2L_p$ is chosen, the first radiating mode does become TM_{20}.

To achieve the resonance of TM_{01} at the desired 5.8 GHz it must be, theoretically from Eq. (1), $L_p = 11.75$ mm. This first antenna, hereinafter referred to as p#1, has been etched on FR408 ($\varepsilon_r = 3.6$, $\tan\delta = 0.0127$, thickness 1.6 mm) and has the geometry in Figure 1(a) and the dimensions tuned via a full wave simulation to achieve the desired working frequency of 5.8 GHz reported in Table 1 (the first column). Figure 2 shows the simulated 2D electric field map for this antenna, clearly showing the TM_{01} distribution.

With p#1 being the width set at $W_p \simeq 1.5L_p$, there is no degeneracy, and the correct mode TM_{01} is excited. Figure 2 confirms this, showing uniform electric field along the long edges, hence the maximum radiated field is in the broadside direction.

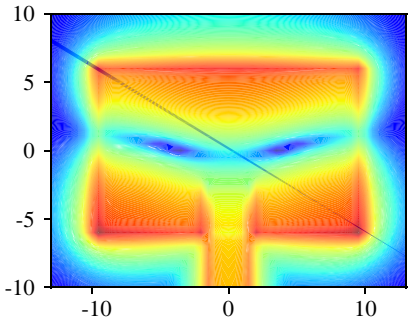

Figure 2. 2D map of electric field distribution for patch p#1 at 5.8 GHz.

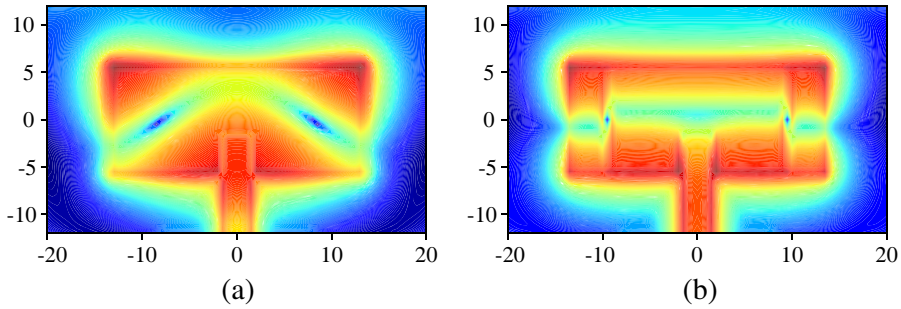

Figure 3. 2D maps of electric field distribution at 5.8 GHz. (a) shows fields for the p#2 design; (b) shows fields for the p#3 designed where a pair of slots, whose effect is clearly visible, is used to suppress the TM_{20} mode.

In Figure 3, the field-map on the left shows the electric filed distribution for a second patch, referred to as p#2, which is similar to p#1 except that now $W_p \simeq 2L_p$, with other quantities being slightly tuned to try to maintain the matching (Table 1 second column — indeed matching is extremely poor as will be shown later). The field is apparently distorted by the superimposition of the undesired TM_{20} mode onto the desired TM_{01}. The radiation is consequently impaired.

Since the gain of a patch is related to its overall dimension, this behaviour causes a limit to the achievable maximum gain. In order to overcome this restriction and keep both matching and maximum radiated field in the broadside direction, a pair of slots optimized in size and position are exploited.

It is fairly well known that TM_{01} has only $H_x \neq 0$ in the cavity, according to the reference in Figure 1, which implies y-directed surface currents on the patch. On the other hand, TM_{20} has only $H_y \neq 0$ in the cavity, which implies x-directed surface currents on the patch.

Hence the addition of a pair of slots as in Figure 1(b) does not perturb the TM_{01} mode significantly while severely interfering the TM_{20} currents. The optimal set of parameters for the slots minimizing return loss and maximizing the feed can be obtained with a multi-objective approach, like [11, 12] and leads to a design which will be referred to as p#3 in the following section.

Hence, the design in Table 1 (third column) is achieved. Figure 3(b) shows the electric field distribution of such a design. It is evident how the presence of the two slots forces the electric field on the radiating edge to be uniform, due to the presence of only the TM_{01} mode, hence maximizing gain.

3. EXPERIMENTAL VALIDATION

In this section, the experimental validation of the proposed antenna is provided.

Figure 4 shows p#2 and p#3 antenna prototypes printed by photo-etching procedure on a commercial "off-the-shelf" FR408 substrate ($\varepsilon_r = 3.6$, $\tan\delta = 0.01$, thickness = 1.6 mm). The prototypes characterization is carried out with a Keysight N5242A VNA working in the 10 MHz–

Table 1. Patches dimensions in mm (N.A. stands for not applicable to a given geometry).

	p#1	p#2	p#3
W	48	48	48
L	25	25	25
W_p	18.15	26.95	26.95
L_p	12.15	11.75	11.75
g_s	N.A.	N.A.	0.3
d_1	N.A.	N.A.	3.78
d_2	N.A.	N.A.	0.2
w	3.1	3.1	3.1
g_a	0.25	0.5	0.25
d_a	3.8	4.5	4.5

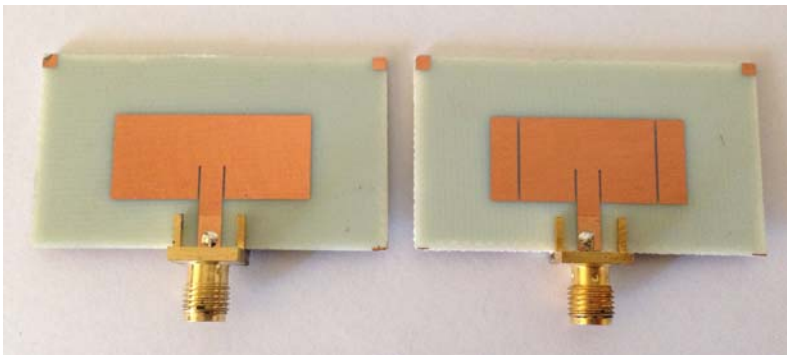

Figure 4. Prototype of the p#2 antenna, on the left; prototype of the p#3 antenna (on the right).

26.5 GHz range with the antenna placed in our anechoic chamber and connected via standard SMA-connectorized coaxial cables. Two identical antennas are used for transmitting and receiving for easier characterization of patterns and gains. The comparison between measurement and simulation is depicted in Figures 5 and 6 for what concerns gain patterns and in Figure 7 for what concerns matching.

In order to gain a better insight on achieved performances, a fourth structure, p#4, has been analyzed — at a simulation level only. This last structure is an array of two patches p#1, whose centers are at a mutual distance equal to $\lambda/2$. Obviously, this is by far the largest of the structures, and it also has a higher gain, but due to higher losses in the feeding network, its gain is anyway comparable to that of p#3. In application where compactness of the structure is a critical requirement, p#3 results in a better choice. Indeed, p#4 is not only larger because of the two patches, but also wider due to the

Table 2. Size and performances comparison between the different designs (N.D. stands for not definable; N.R. stands for not realized).

antenna	$L \times W$ [mm^2]	B [%]	G [dB]	RG [dB]
p#1	25×48	4.8	5.06	N.R.
p#2	25×48	N.D.	5.05	4.83
p#3	25×48	3.9	7.12	6.85
p#4	37.5×69.9	4.8	7.3	N.R.

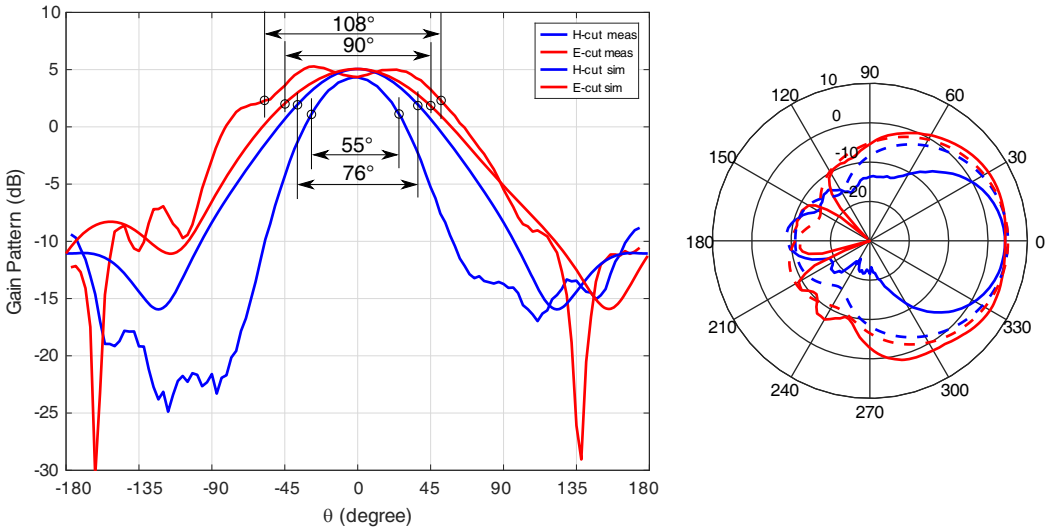

Figure 5. Simulated and Measured gain for patch p#2. Half power (−3 dB) beamwidth are also highlighted.

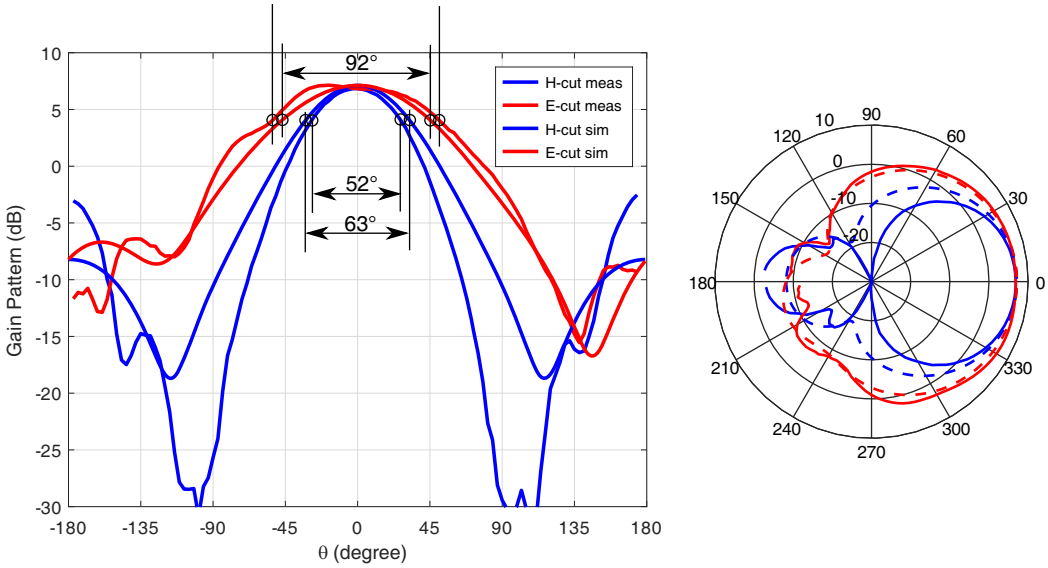

Figure 6. Measured gain for patch p#3. Half power (−3 dB) beamwidth are also highlighted.

corporate feed, as shown in Table 2, where the comparison in terms of overall dimensions, bandwidth, and gain are reported.

Patch p#3 realizes a gain comparable to that of the two-patch array p#4 although its area is about half of that of p#4. In addition, with respect to p#1, antenna p#3 presents a gain better than about 2 dB in spite of its bandwidth with its dimension being substantially the same as p#1. For patch p#2, −10 dB bandwidth cannot be defined since due to the extremely poor matching, 10 dB return loss is never reached, as shown in Figure 7, representing the reflection coefficient at the antenna feeding port.

Half power beamwidth (HPBW) can, on the other hand, be defined on both antennas, and both on simulations and measurements. Values are reported in Figures 5 and 6. HPBW is smaller on H-plane than on E-plane for both designs as expected, and measured results show a further — indeed welcome — reduction on H-plane and corresponding augmentation on E-plane due to non-idealities and tolerances in manufacturing.

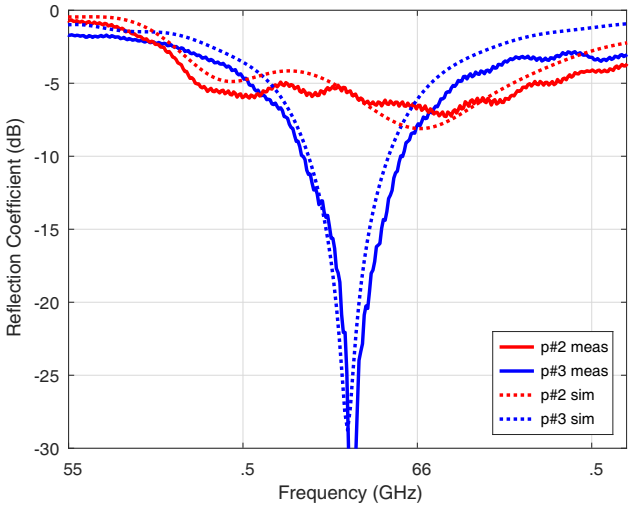

Figure 7. Reflection coefficient for the two antennas under test: p#2 and p#3. It is apparent how p#2 is badly mismatched due to the presence of two resonant modes.

4. CONCLUSIONS

A rectangular patch antenna suitable for Dedicated Short Range Communication in the C-band is designed, analyzed, and fabricated. The antenna is based on a single-layer via-less design, consisting of a rectangular patch etched with a pair of thin slots. These slots inhibit higher modes, permitting a large resonant edge.

The experimental validation demonstrates the effectiveness of the proposed approach for the design, which attains a realized gain 6.85 dB. Such realized gain is 2 dB higher with respect to the reference resonant patch, whose realized gain is 4.83 dB, and comparable with that of a two element array which, on the other hand, is much larger. Furthermore, the desired narrow H-plane HPBW and wide E-plane HPBW are achieved, allowing correct illumination of a single lane.

REFERENCES

1. ES200674-1 V1.2.I, "Electromagnetic compatibility and Radio Spectrum Matters (ERM); Road Transport and Traffic Telematics (RTTT); Part 1: Technical characteristics and test methods for High Data Rate (HDR) data transmission equipment operating in the 5, 8 GHz Industrial, Scientific and Medical (ISM) band," ETSI, 2007.
2. Cidronali, A., S. Maddio, M. Passafiume, and G. Manes, "Car talk: Technologies for vehicle-to-roadside communications," *IEEE Microwave Magazine*, Vol. 17, No. 11, 40–60, 2016.
3. Inserra, D., W. Hu, and G. Wen, "Planar antenna array design considerations for RFID electronic toll collection system," *2016 IEEE MTT-S International Wireless Symposium (IWS)*, 1–4, IEEE, 2016.
4. Joshi, M. P. and V. J. Gond, "Design and analysis of microstrip patch antenna for WLAN and vehicular communication," *Progress In Electromagnetics Research*, Vol. 97, 163–176, 2019.
5. Inserra, D., W. Hu, and G. Wen, "Antenna array synthesis for RFID-based electronic toll collection," *IEEE Transactions on Antennas and Propagation*, Vol. 66, No. 9, 4596–4605, 2018.
6. Maddio, S., G. Pelosi, M. Righini, and S. Selleri, "A compact series array for vehicular communication in the C-band," *2019 IEEE International Symposium on Antennas and Propagation and USNC-URSI Radio Science Meeting*, 1337–1338, IEEE, 2019.
7. Haran, M., G. Dilip Kumar, A. Ferris Garvin, and S. Ramesh, "Hexagonal microstrip patch antenna for early stage skin cancer identification," *Telecommunications and Radio Engineering*, Vol. 79, No. 7, 555–566, 2020.

8. Ebenezer Abishek, B., A. Raaza, S. Ramesh, S. Jerritta, and V. Rajendran, "Circularly polarized circular slit planar antenna for vehicular satellite applications," *Applied Computational Electromagnetics Society Journal*, Vol. 34, No. 9, 1340–1345, September 2019.
9. Garg, R., *Microstrip Antenna Design Handbook*, Artech House, 2001.
10. James, J. R., P. S. Hall, et al., *Handbook of Microstrip Antennas*, Vol. 1, IET, 1989.
11. Agastra, E., G. Pelosi, S. Selleri, and R. Taddei, "Taguchi's method for multi-objective optimization problems," *International Journal of RF and Microwave Computer-Aided Engineering*, Vol. 23, No. 3, 357–366, 2013.
12. Pelosi, G., S. Selleri, and R. Taddei, "A novel multiobjective Taguchi's optimization technique for multibeam array synthesis," *Microwave and Optical Technology Letters*, Vol. 55, No. 8, 1836–1840, 2013.